Electrocatalytic Oxidation and Sensitive Detection of Cysteine on a Lead Ruthenate Pyrochlore Modified Electrode

ARTICLE *in* ANALYTICAL CHEMISTRY · FEBRUARY 2001

Impact Factor: 5.64 · DOI: 10.1021/ac0010781

3 AUTHORS, INCLUDING:

Jyh-Myng Zen
National Chung Hsing University
167 PUBLICATIONS **3,668** CITATIONS

SEE PROFILE

Annamalai Senthil Kumar
VIT University
129 PUBLICATIONS **2,123** CITATIONS

SEE PROFILE

Anal. Chem. **2001,** *73,* 1169−1175

Electrocatalytic Oxidation and Sensitive Detection of Cysteine on a Lead Ruthenate Pyrochlore Modified Electrode

Jyh-Myng Zen,* Annamalai Senthil Kumar, and Jyh-Cheng Chen

Department of Chemistry, National Chung-Hsing University, Taichung 402, Taiwan

Electrocatalytic oxidation of cysteine (CySH) at Nafion/lead ruthenate pyrochlore (*Py*) chemically modified electrodes was thoroughly studied. Electrochemical ac impedance spectroscopy analysis indicated the formation of *Py* microparticles in the interfacial galleries of Nafion. Experiments with benchmark systems of $Fe(CN)_6^{3-/4-}$ and $Ru(bpy)^{2+/3+}$ reveal the suppression of Nafion's anionic character after the in situ precipitation of *Py*. Michaleis−Menten-type kinetics with the rate determination step of CyS−*Py*−Ru^{VI} → *Py*−Ru^{IV} + CyS−SCy was proposed for this catalytic oxidation. The electrocatalytic behavior is further developed as a sensitive detection scheme for CySH by square-wave voltammetry (SWV) and flow injection analysis (FIA). Under the optimized conditions, the calibration curve is linear up to 560 μM with a detection limit (signal/noise 3) of 1.91 μM in SWV. The detection limit can be improved to 1.70 nM (i.e., 24.22 ng in a 20-μL sample loop) in FIA. This is the lowest value ever reported for direct CySH determination without preliminary accumulation.

The sulfur-containing molecule cysteine (CySH) plays a crucial role in biological systems, especially in folding and defolding mechanisms.[1] Because CySH possesses a very low molar extinction coefficient, a spectroscopic method is suitable for its detection only with derivatization via the sulfhydryl functionality.[2] Compared to other options, electroanalysis has the advantage of simplicity and high sensitivity. Several electrochemical systems, such as Nafion/$Os(bpy)_3^{2+}$, polycrystalline gold, vitamin B_{12}-adsorbed graphite, phthalocyanine (Pc) complexes of Co and Mo, water-soluble Fe and Mn porphyrins, and Ni−Pc immobilized silica gel-modified TiO_2 (ST-NiTsPc) electrodes, were reported for CySH detection.[3−10] Unfortunately, most electrodes contain certain disadvantages to extend them into real application. For example, the Nafion/$Os(bpy)_3^{2+}$ electrode showed considerable leaching of $Os(bpy)_3^{2+}$ even after it was stabilized in Nafion film.[3] The oxidation process of CySH on polycrystalline gold electrode displayed complicated kinetics and the irreversible adsorption behavior rendered the routine analysis difficult.[4] Although the Pc complexes possess substantial catalytic activity, there is a solubility problem in an acidic environment. The ST-NiTsPc/carbon paste electrode was reported recently to overcome these problems except that the detection range (1−7 mM) is not sensitive enough for real-sample analysis and the interference from other biological chemicals is considerably high.[10]

Surprisingly, metallic oxide electrodes have hardly been used for this purpose, although they possess redox groups with tunable oxidation state and large surface area. Ruthenium dioxide (RuO_2) has been reported to have excellent electrocatalytic activity toward a number of organic compounds through mediation by Ru(VII)/Ru(VI), Ru(VI)/Ru(IV), or Ru(IV)/Ru(III) redox couples.[11−21] Nevertheless, the high-temperature pyrolysis (300−700 °C) route in preparation and large double-layer charging effect make RuO_2 less favorable for analytical applications.[19−21] To overcome the main drawbacks of conventional RuO_2 electrodes, we disclosed a Nafion/lead ruthenate pyrochlore (*Py*) chemically modified electrode (designated as N*Py*CME) in electrocatalytic application with excellent sensitivity.[22−34] In this paper, we report the detail and

* To whom correspondence should be addressed. Fax: 886-4-2862547. E-mail: jmzen@dragon.nchu.edu.tw.

(1) Voet, D.; Voet, J. G. *Biochemistry*, 2nd ed.; John Wiley & Sons: New York, 1995; p 1263.
(2) Chwatko, G.; Bald, E. *Talanta* **2000**, *52*, 509−515.
(3) Chen, X.; Xia, B.; He, P. *J. Electroanal. Chem.* **1990**, *281*, 185−198.
(4) Fawcett, W. R.; Fedurco, M.; Kovacova, Z.; Borkowska, Z. *J. Electroanal. Chem.* **1994**, *368*, 265−274.
(5) Zagal, J. H.; Aguirre, M. J.; Parodi, C. G. *J. Electroanal. Chem.* **1994**, *374*, 215−222.
(6) Li, H.; Li, T.; Wang, E. *Talanta* **1995**, *42*, 885−890.
(7) Halbert, M. K.; Baldwin, R. P. *Anal. Chem.* **1985**, *57*, 591−595.
(8) Mafatle, T. J.; Nyokong, T. *J. Electroanal. Chem.* **1996**, *408*, 213−218.
(9) Chen, S.-M. *Electrochim. Acta* **1997**, *42*, 1663−1673.
(10) Perez, E. F.; Kubota, L. T.; Tanaka, A. A.; De Oliveira Neto, G. *Electrochim. Acta* **1998**, *43*, 1665−1673.
(11) Burke, L. D.; Murphy, O. J. *J. Electroanal. Chem.* **1979**, *101*, 351−361.
(12) Burke, L. D.; Healy, J. F. *J. Electroanal. Chem.* **1981**, *124*, 327−332.
(13) O'Sullivan, E. J. M.; White, J. R. *J. Electrochem. Soc.* **1989**, *136*, 2576−2583.
(14) Shieh, D.-T.; Hwang, B.-J. *J. Electrochem. Soc.* **1995**, *142*, 816−823.
(15) De Andrade, A. R.; Donate, P. M.; Alves, P. P. D.; Carlos, H. V. F. *J. Electrochem. Soc.* **1998**, *145*, 3839−3843.
(16) Leech, D.; Wang, J.; Smyth, M. K. *Analyst* **1990**, *115*, 1447−1450.
(17) Lyons, M. E. G.; Lyons, C. H.; Michas, A.; Bartlett, P. N. *Analyst* **1994**, *119*, 855−861.
(18) Wang, J.; Taha, Z., *Anal. Chem.* **1990**, *62*, 1413−1416.
(19) Trasatti, S. In *Electrochemistry of Novel Materials*; Lipkowski, J., Ross. P. N., Eds.; VCH Publishers: New York, 1995; p 207.
(20) Senthil Kumar, A. Ph.D. Thesis, University of Madras, Alagappa College of Technology, Madras, India, 1998.
(21) Senthil Kumar, A.; Chandrasekara Pillai, K. *J. Solid State Electrochem.* **2000**, *4*, 408−416.
(22) Zen, J.-M.; Wang, C.-B. *J. Electrochem. Soc.* **1994**, *141*, L51−L52.
(23) Zen, J.-M.; Wang, C.-B. *J. Electroanal. Chem.* **1994**, *368*, 251−256.
(24) Zen, J.-M.; Tang, J.-S. *Anal. Chem.* **1995**, *67*, 208−211.
(25) Zen, J.-M.; Tang, J.-S. *Anal. Chem.* **1995**, *67*, 1892−1895.
(26) Zen, J.-M.; Ting, Y.-S. *Anal. Chim. Acta* **1997** *342*, 175−180.

10.1021/ac0010781 CCC: $20.00
Published on Web 02/15/2001

systematic investigation for the catalytic mechanism of CySH oxidation at the N*Py*CME. Electrochemical impedance spectroscopy (EIS) provides insight information about the formation of *Py* particles inside the Nafion membrane. The catalytic mechanism was further applied in the determination of CySH at trace level by square-wave voltammetry (SWV) and flow injection analysis (FIA). An extraordinary sensitivity for CySH was obtained at the N*Py*CME by FIA.

EXPERIMENTAL SECTION

Chemicals and Reagents. DL-Cysteine (99%), cystine, *N*-acetylcysteine, glutathione, glycine, Nafion perfluorinated ion-exchange powder, 5 wt % solution in a mixture of lower aliphatic alcohols and 10% water, lead nitrate, ruthenium trichloride, $K_3[Fe^{III}(CN)_6]$, and $[Ru^{II}(bpy)_3]Cl_2$ were all obtained from Aldrich (Milwaukee, WI). All the other compounds (ACS-certified reagent grade) were used without further purification. Aqueous solutions were prepared with doubly distilled deionized water.

Apparatus. Cyclic voltammetry (CV) and SWV were performed on a BAS 100B electrochemical analyzer and a BAS VC-2 electrochemical cell (West Lafayette, IN). The three-electrode system consisted of a N*Py*CME working electrode, an Ag/AgCl reference electrode, and a platinum wire auxiliary electrode. Since oxygen did not interfere with the voltammetric analysis of CySH, no deaeration was performed for qualitative and quantitative determinations. The EIS measurements were performed using an Autolab frequency response analyzer with FRA2 module that was controlled by an IBM-compatible PC. It was measured at 10 discrete frequencies per decade from 0.01 to 10^5 Hz with 5-mV amplitude at an applied bias potential of 0.8 V versus Ag/AgCl. An in-house built FRA2 software fitting program was used for circuit analysis. A wall-jet-type working system was used in FIA. This consisted of a Cole-Parmer microprocessor pump drive, a Rheodyne model 7125 sample injection valve (20-μL loop) with interconnecting Teflon tube, and a BAS electrochemical detector. A carrier solution of pH 7.4 phosphate-buffer solution (PBS; I = 0.1 M) was used throughout the FIA experiments. UV−visible spectra were recorded with a Hitachi U-3000 spectrophotometer.

Procedures. The N*Py*CME was prepared as described previously.[23] Briefly, the Nafion-coated GCE (designated as Nafion-GCE) was first formed by spin-coating with 4 μL of 4 wt % Nafion solution at 3000 rpm. The Nafion-GCE was then ion-exchanged with Ru^{3+} and Pb^{2+} and further reacted in 1.1 M KOH at 53 °C for 24 h with constant purging of O_2. The preparation procedure resulted in uniform distribution of the catalytically active microparticles throughout the Nafion matrix. The formation of *Py* inside the Nafion film was confirmed by the X-ray diffraction pattern in our previous study.[23] As to the preparation of the Nafion/*Py* composite electrode (designated as N*Py*CE), 4 wt % Nafion was mixed with 1.5 μg/cm^2 *Py* powder and 4 μL of this mixture was spin-coated on a clean GCE. The *Py* powders were prepared according to the procedure reported earlier.[31]

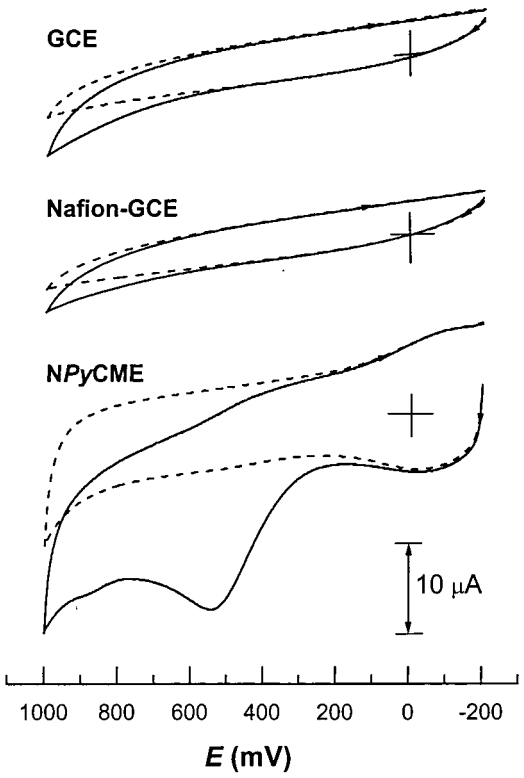

Figure 1. Cyclic voltammograms with (solid lines) and without (dotted lines) 1 mM CySH at different electrodes in pH 7.4 PBS at a scan rate of 50 mV/s.

SW voltammograms were obtained by scanning the potential from 0.3 to 1.0 V at a frequency and amplitude of 25 Hz and 55 mV, respectively. At a step height of 4 mV, the effective scan rate is 100 mV/s. The CySH quantification was achieved by measuring the oxidation peak current. Unless otherwise mentioned, 0.1 M, pH 7.4 PBS was used for all electrochemical measurements.

RESULTS AND DISCUSSION

Voltammetric Study. Figure 1 shows the CV responses of 1 mM CySH on a bare GCE, Nafion-GCE, and N*Py*CME in pH 7.4 PBS at a scan rate of 50 mV/s. As can be seen, only at the N*Py*CME was an anodic peak corresponding to the oxidation of CySH to CyS−SCy observed.[32] This result clearly demonstrates the effective catalytic behavior of the N*Py*CME. The absence of the corresponding cathodic peak indicates the irreversible nature of the CySH oxidation process. It is surprising that there is no obvious faradaic behavior on the N*Py*CME in bare electrolyte. It may be due to very low oxide content (i.e., loading) by in situ precipitation or due to the highly porous and amorphous nature of *Py* in the Nafion film. Nevertheless, the *Py* particles can still show their specific catalytic activity. Similar behavior was also noticed on PVC/*Py* and Nafion/*Py* composite electrodes, which are not prepared by in situ precipitation procedure like N*Py*CME.[31]

The plot of $\log(i_{pa})$ versus $\log(v)$ yielded a slope very close to 0.5 on the N*Py*CME, suggesting that the oxidation follows a diffusion-controlled charge-transfer mechanism with a current function, $i_{pa}/(v^{1/2}C_{CySH})$, of 54.01 A V$^{-1/2}$ s$^{1/2}$ mol^{-1} cm^3. On the basis of $E_{pa} = [b_a\log(v)]/2 +$ constant, for a totally irreversible

(27) Zen, J.-M.; Ting, Y.-S. Shih, Y. *Analyst* **1998**, *123*, 1145−1147.
(28) Zen, J.-M.; Chang, M.-R.; Ilangovan, G. *Analyst* **1999**, *124*, 679−684.
(29) Zen, J.-M.; Lai, Y.-Y.; Ilangovan, G.; Senthil Kumar, A. *Electroanalysis* **2000**, *12*, 280−286.
(30) Zen, J.-M.; Senthil Kumar, A.; Chang, M.-R. *Electrochim. Acta* **2000**, *45*, 1691−1699.
(31) Zen, J.-M.; Senthil Kumar, A.; Chen, J.-C. *J. Mol. Catal. A* **2001**, *165*, 177−188.
(32) Zen, J.-M.; Senthil Kumar, A.; Chen, J.-C. *Chem. Lett.* **1999**, *8*, 743−744.
(33) Zen, J.-M.; Senthil Kumar, A.; Chen, J.-C. *Electroanalysis*, in press.
(34) Zen, J,-M.; Senthil Kumar, A.; Wang, H.-F. *Analyst* **2000,** *125*, 2169−2172.

Scheme 1. Electrocatalytic Mediated Mechaism for CySH Oxidation at the N*Py*CME[a]

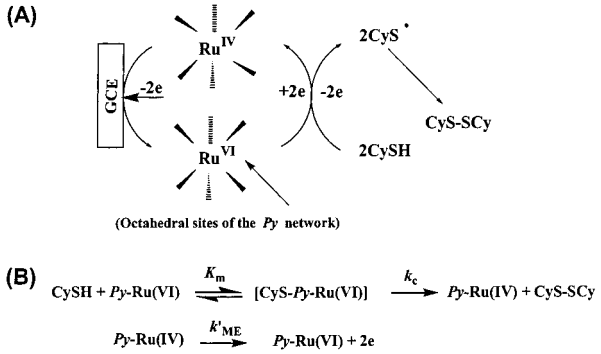

[a] (A) Illustration of the partcipation of the *Py*−$Ru^{VI/IV}$ redox sites in the mediated mechanism. (B) Reaction pathway based on the Michaelis−Menten kinetics.

diffusion-controlled process,[35,36] the b_a (i.e., Tafel slope) value is measured as 30.3 mV/decade. Assuming one-electron transfer in the rate determination step (i.e., $n_a = 1$), since $b_a = 2.303RT/n_aF\alpha_a$, the anodic-transfer coefficient (α_a) can then be calculated as 0.99. This indicates the effective catalytic performance of the N*Py*CME. The i_{pa} versus [CySH] plot at a quasi-steady-state condition (i.e., at $v = 10$ mV/s) yielded a straight line up to 40 mM and then reached a plateau. This behavior follows surface saturation kinetics, which is close to the operation of a Michaelis−Menten-type reaction mechanism.[17] The reaction order, m, was estimated as 0.94 from the $\log(i_{pa})$ versus log[CySH] plot and the value is close to the Michaelis−Menten prediction.[17,29]

Our preliminary report has demonstrated the Michaelis−Menten kinetics and its corresponding basic mechanistic parameters, such as catalytic (k_c), electrochemical (k'_{ME}), and Michaelis−Menten (K_m) rate constants.[32] These data were evaluated from the Lineweaver−Burke (LB) analysis, and some of the results were compared to a recent report on the ST-NiTsPc electrode.[10,32] Scheme 1 shows the electrocatalytic oxidation mechanism of CySH to CyS−SCy through the *Py*−Ru^{VI}/Ru^{IV} redox couple. In the electrocatalytic pathway, the reaction of CyS−*Py*−$Ru^{VI} \rightarrow$ *Py*−Ru^{IV} + CyS−SCy is considered as the rate determination step (rds) with a rate constant (k_c) of 6.33 s^{-1}.[32] Note that CyS−*Py*−Ru^{VI} is a high-energy intermediate complex close to the Eryings activated complex and it is difficult to trap either by electrochemical and spectroscopic techniques.[29] On the other hand, the physical picture regarding its equilibrium kinetics can be seen from the Michaelis−Menten rate constant (K_m). The UV−visible spectrum of the electrochemically (ec) oxidized products in pH 4 and 7 confirms the overall basic mechanism as illustrated in Scheme 1. It is performed by injecting a small volume of 1 mM CySH at 1.1 V, and a specific peak at $\lambda_{max} = 283$ nm was observed. This absorption wavelength is identical to the characteristics of −S−S− link as reported earlier.[37,38]

The *Py* trapped in the interfacial sites of the Nafion galleries is expected to be responsible for the electrocatalytic oxidation. Experiments with benchmark model systems of anionic

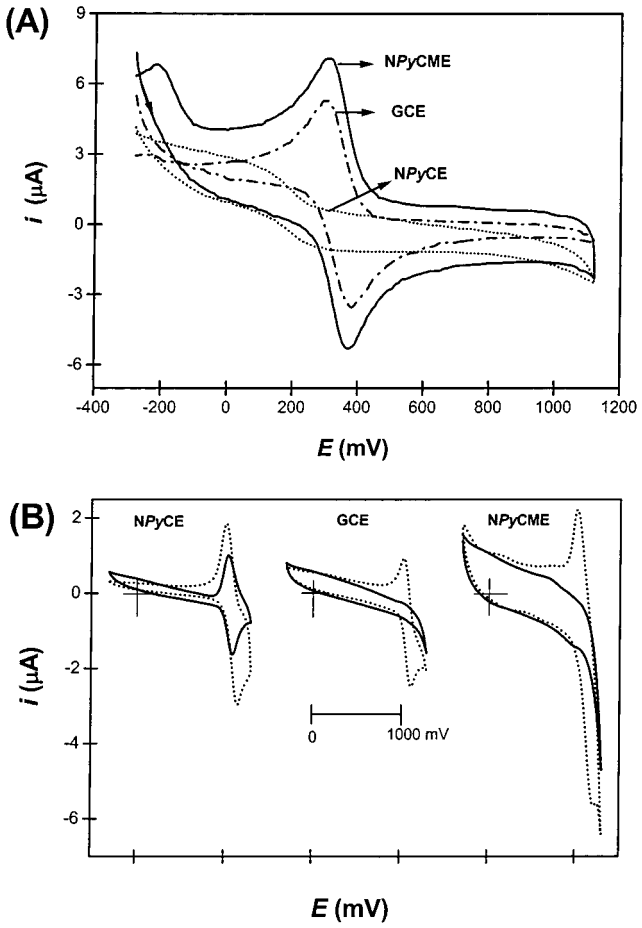

Figure 2. Electron-transfer reaction with benchmark model systems. (A) CV responses on different electrodes with 5 mM $Fe(CN)_6^{3-/4-}$ at $v = 10$ mV/s. (b) CV responses in 1 mM $Ru(bpy)_3^{2+/3+}$ at $v = 50$ mV/s before (dashed line) and after (solid line) transfer to the pure base electrolyte solution.

$Fe(CN)_6^{3-/4-}$ and cationic $Ru(bpy)_3^{2+/3+}$ indicate the malfunction of the ion-exchange ability of Nafion at the N*Py*CME. Figure 2A shows the typical CV response of 5 mM $Fe(CN)_6^{3-/4-}$ with the GCE, N*Py*CME, and N*Py*CE at $v = 10$ mV/s. Due to the strong repulsion effect of Nafion with $Fe(CN)_6^{3-/4-}$, a poor CV behavior was observed on the N*Py*CE. The CV response at the N*Py*CME, however, showed as clear and sharp redox signal as that at GCE. The absence of repulsion effect indicates that the cationic sites of Nafion are occupied by *Py* units in the N*Py*CME. Further evidence was provided by studying with cationic $Ru(bpy)_3^{2+/3+}$ complex at $v = 50$ mV/s as shown in Figure 2B. In all cases, before transfer to its blank solution, a well-defined anodic peak of $Ru(bpy)_3^{2+/3+}$ at 1.10 V was noticed. However, only the N*Py*CE still shows a peak response after transfer to blank solution. This result again proves the absence of cationic exchange ability of Nafion at the N*Py*CME.

EIS Study. The purpose of EIS studies is to pursue insight regarding the *Py* formation and the film resistivity. Supporting evidence for the in situ crystallization of *Py* and its physical properties in the N*Py*CME can also be obtained from this study. Figure 3 shows the complex plane plots for the Nafion-GCE and N*Py*CME with/without 1 mM CySH at a bias potential of 0.8 V in a wide frequency range of $0.01-10^5$ Hz. Both electrodes were found to follow a similar trend in blank electrolyte except that

(35) Xia, H.; Li, H.-L., Z. *J. Electroanal. Chem.* **1997**, *430*, 183−187.
(36) Golabi, S. M.; Zare, H. R. *J. Electroanal. Chem.* **1999**, *465*, 168−176.
(37) Clevland, W. W. *Biochemistry* **1964**, *3*, 480−482.
(38) Morioka, Y.; Kobayashi, K. *Biol. Pharm. Bull.* **1997**, *20*, 825−827.

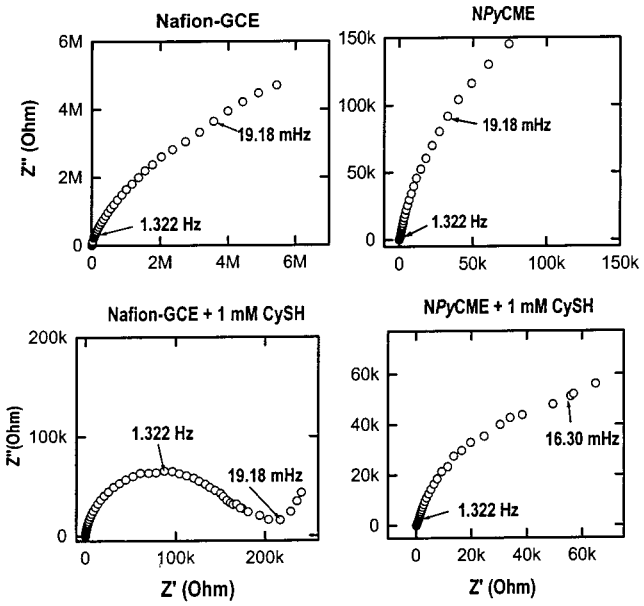

Figure 3. Complex plane plots for different electrodes with and without 1 mM CySH at an applied bias potential of 0.8 V versus Ag/AgCl in pH 7.4 PBS.

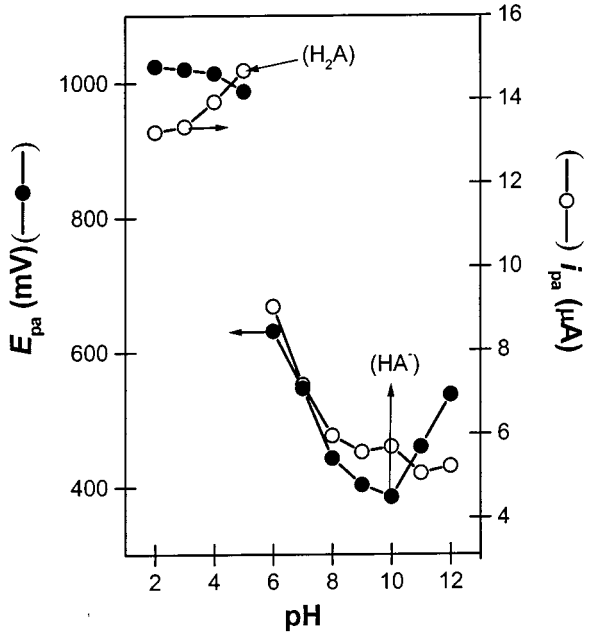

Figure 4. Plots of E_{pa} and i_{pa} versus pH for 1 mM CySH on the N*Py*CME using CV in different pHs at $v = 50$ mV/s.

the resistance in Ω was dramatically lowered by ~3 orders for the N*Py*CME. Obviously, it is due to the existence of conducting crystallite catalysts inside the interfacial sites of the Nafion matrix. The complex plane plot is dramatically different between the Nafion-GCE and N*Py*CME in the presence of CySH. A semicircle with a frequency maximum at 1.322 Hz was observed at the Nafion-GCE. Whereas, a broad and distorted semicircle curve at a comparatively lower Ω value was noticed on the N*Py*CME. Simple semicircle analysis, using the Boucamp circuit of $R_s(R_{ct}C_{dl})$, shows calculated values of $R_{ct} = 1.719 \times 10^5$ Ω, $C_{dl} = 59.06$ nF, and $n = 0.83$ for the Nafion-GCE with CySH. In the circuit, R_s, R_{CT}, and C_{dl} represent solution resistance, faradaic charge-transfer resistance, and double-layer capacitor, respectively. Note that, $n = 1$ indicates a pure capacitative behavior of the C_{dl}. These results show the sluggish faradic electron transfer with high resistance of CySH on the Nafion-GCE as shown in Figure 1 and Figure 3. On the other hand, the EIS analysis confirms the formation of *Py* microparticles in the interfacial galleries of Nafion. The lowering in resistivity of the film can in turn mediate the electrocatalytic oxidation of CySH. The obtained EIS plot for the N*Py*CME with CySH is not a Randle-type semicircle behavior and is different from that of GCE and Nafion-GCE. Thus, we believe the N*Py*CME has a complex internal electrical circuit. Detailed EIS analysis on the above electrode is necessary to solve this problem.

Effect of pH. Figure 4 shows the effect of pH on the CV response of 1 mM CySH on the N*Py*CME. As can be seen, no simple increase in E_{pa} versus pH was observed and relatively higher i_{pa} was noticed when pH was <5. The behavior is very different from uric acid and norepinephrine (NE) and other organic compound oxidation on the N*Py*CME with a linear increase in E_{pa} versus pH.[25,31,33] The discrepancy has something to do with CySH since it contains various functional groups of COOH, SH, and NH_2 with pK_a of 1.71, 8.36, and 10.77, respectively (Figure 5A).[39] The SH group possesses the strongest oxidizing tendency among the three functional groups and can form the disulfide (CyS−SCy) bond easily. To our knowledge, there is no specific study about the dissociation (i.e., speciation) of CySH so far. We deconvoluated the different chemical species of CySH against pH using simple chemical equilibrium analysis as shown in Figure 5B.[40] As can be seen, the dominant species change with pH and can be used to explain the experimental results. For example, an increasing trend in the pH range of 6−10.77 was reported on a vitamin B_{12}-adsorbed OPG electrode toward CySH oxidation.[5] On the basis of the distribution diagram, the responsible species in this case is [HA^-], i.e., CyS^-. The N*Py*CME shows maximum current values at pH <5 and thus the cationic [H_3A^+] (i.e., $CySH_2^+$) or the neutral [H_2A] (i.e., CySH) is responsible for the disulfide formation and can be explained as follows.

For metallic oxides, the surface hydroxyl groups play an essential role for the electrocatalytic reactions.[19−21,31,41−43] The reported pH_{PZC} for *Py* is ~4.0, and the oxide surface is acidic when pH is <4 and basic when pH is >4.[31,43] It is therefore expected that the acidic surface sites are responsible for the enhanced disulfide formation. Indeed, sulfur-containing ligands were reported to lead to an effective catalytic activity on acidic surface sites of metallic oxides.[41] Considering the electronegativity of O (3.5) > N (3.0) > S (2.5), the oxygen-containing terminals should directly face the acidic surface sites and either N or S sites are loosely coordinated to the high-valence metal ions. To check the expectation, parallel experiments were carried out using glu-

(39) *The Merk Index*, VIth ed.; Merck & Co. Inc.: Rahway, NJ, 1989.
(40) Rubinson, K. A. *Chemical Analysis*; Little, Brown and Co.: Boston, 1987; p 34.
(41) Ziolek, M.; Kujawa, J.; Saur, O.; Lavalley, J. C. *J. Mol. Catal. A* **1995**, *19*, 49−55.
(42) Goodenough, J. B.; Manoharan, R.; Paranthaman, M. *J. Am. Chem. Soc.* **1990**, *112*, 2076−2085.
(43) Zen, J.-M.; Manoharan, R.; Goodenough, J. B. *J. Appl. Electrochem.* **1990**, *22*, 140−150.

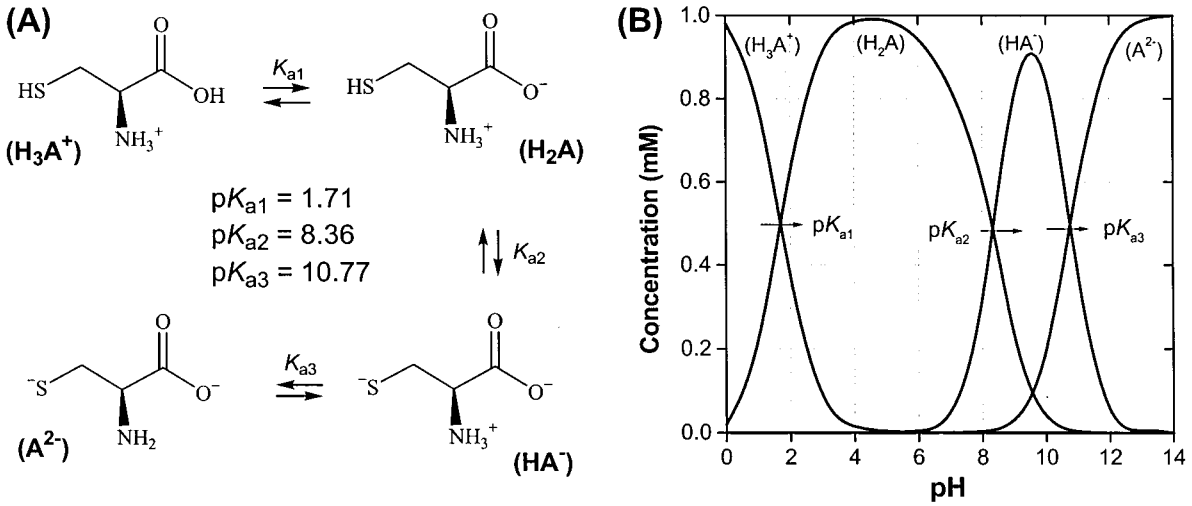

Figure 5. (A) Various forms of CySH with respect to its pK_a value. (B) Distribution curves for various CySH species versus its pH. Distribution curves were simulated for 1 mM CySH.

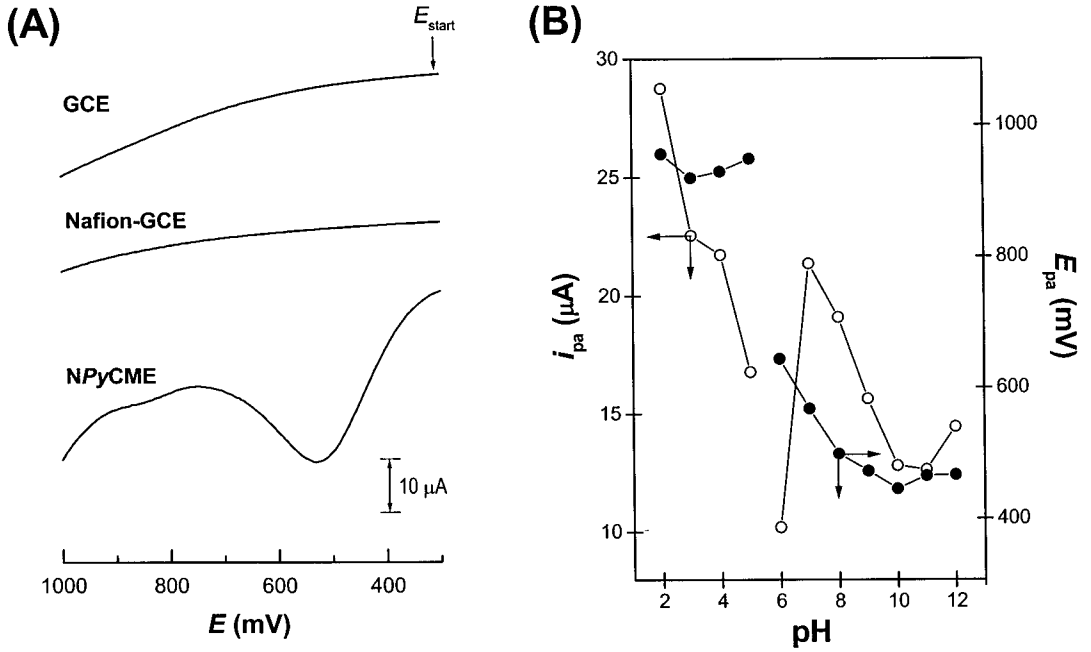

Figure 6. (A) SW voltammograms for 1 mM CySH at different electrodes in pH 7.4 PBS. SWV parameters: amplitude, 55 mV; frequency, 25 Hz; step height, 4 mV. (B) Plots of i_{pa} and E_{pa} versus pH on the N*Py*CME for 1 mM CySH by SWV.

tathione, *N*-acetylcysteine, cystine, and glycine under similar conditions. Interestingly, the obtained qualitative results are similar to that of CySH. On the other hand, no faradaic signals were noticed with glycine and cystine (RS−SR). These observations prove the above expectation that only the SH group alone can get involved in the electrocatalytic oxidation process.

Thus, on the basis of Scheme 1, the irreversible disulfide formation is considered as the rds. The continuous decreasing of i_{pa}, when pH is >5, is a direct indication for the decrease in the overall rate constant (i.e., k_c). In other words, the anionic S^- group can somehow lead to a decrease in k_c. The appearance of two oxidation peaks at 1.0 and 0.5 V at pH 6 confirms the transition of reacting species from SH to S^- on the *Py*−Ru^{VI} sites. Therefore, both the acidic sites of *Py* trapped in Nafion and the SH group are key for the electrocatalytic oxidation process. The electrocatalytic behavior is further utilized as a sensitive detection scheme for CySH at the N*Py*CME.

Analytical Application. Both SWV and FIA were studied and applied for sensitive detection of CySH. Figure 6A shows the typical SWV response for 1 mM CySH on various electrodes. The electrocatalytic effect of the N*Py*CME is qualitatively similar to those of CV results as shown in Figure 1. The effect of pH on the SWV response was first investigated and the i_{pa} and E_{pa} versus pH plots obtained are shown in Figure 6B. As can be seen, the E_{pa} versus pH result is similar to that in Figure 1; whereas, there is an irregular trend at pH 7 for the i_{pa} versus pH result. It may have something to do with the fact that the SWV response is proportional to the reversibility of the system. Nevertheless, this is in effect an advantage considering that the biological reaction takes part in neutral condition. Moreover, it is believed that, at pH 7, the basic electrocatalytic mechanism is the same except with a lower k_c value.

To optimize the SWV response for trace detection of CySH, the corresponding instrumental SWV parameters were studied

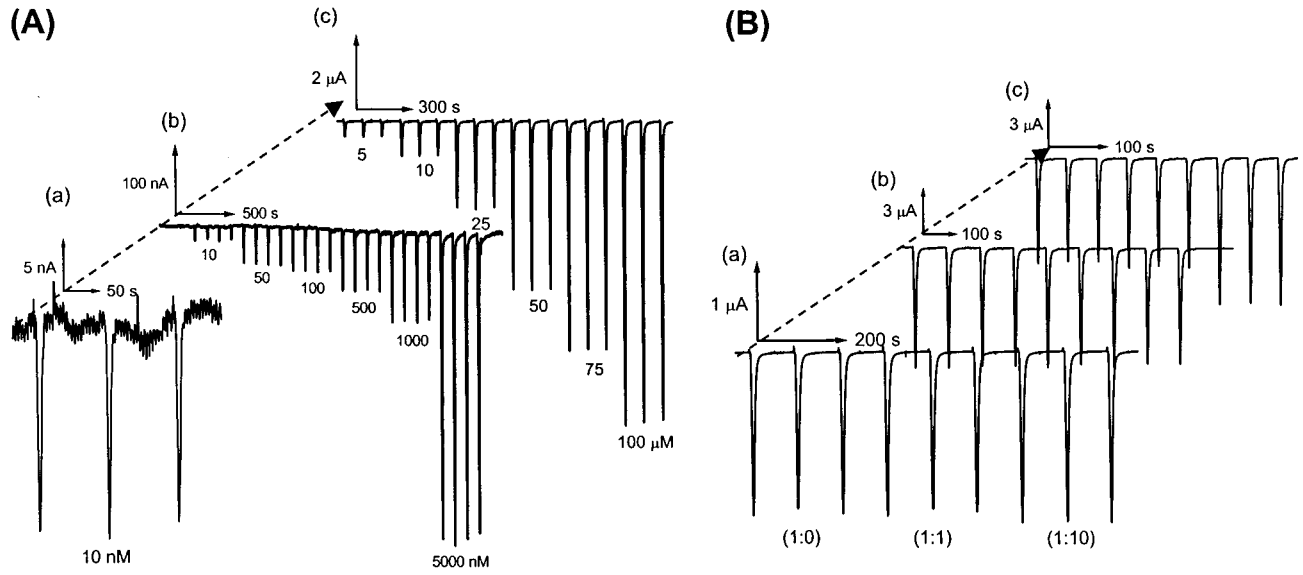

Figure 7. (A) FIA responses for different concentration of CySH (10 nM−100 μM) at the N*Py*CME. Carrier solution was pH 7.4 PBS with a flow rate of 0.30 mL/min and an applied potential of 1.0 V. (B) Interference effect of 1 mM CySH with cystine (a), glucose (b), and oxalic acid (c).

next. These parameters are interrelated and have a combined effect on the response SWV peak, but here only the general trends will be examined. It was found that these parameters had little effect on the peak potential. When the SW amplitude was varied between 10 and 60 mV, the peak currents increased with increasing amplitude. However, the peak width also increased at the same time, in particular when the amplitude was higher than 60 mV. The step height together with the frequency defines the effective scan rate. Hence, an increase with either the frequency or the step height results in an increase in the effective scan rate. The response for CySH oxidation peak current increases with SW frequency up to 25 Hz, above which the peak current was unstable and obscured by a large residual current, in turn decrease in the peak current was noticed. By maintaining the frequency as 25 Hz, the effect of step height was studied. As step height is greater than 4 mV, too few points are sampled, thus affecting the reproducibility of the detection. Overall, the optimized parameters are as follows: preconcentration potential, 0 V; preconcentration time, 20 s; SW frequency, 25 Hz; SW amplitude, 55 mV; step height, 4 mV.

Linear calibration curve is obtained up to 560 μM (67.8 mg/L) with a slope and correlation coefficient of 0.0323 μA/μM and 0.997, respectively, for CySH detection on the N*Py*CME. The detection limit (S/N = 3) is 1.91 μM. To characterize the reproducibility of the N*Py*CME, seven repetitive measurement−regeneration cycles were carried out for 40 and 500 μM CySH. The electrode renewal gives a good reproducible surface since the relative standard deviation obtained was 1.32 and 1.49%, respectively.

It is known that FIA can work with high dead volume with good sensitivity.[44] Experiments regarding hydrodynamic flow rate and applied potential were first systematically optimized as 0.3 mL/min and 1.0 V, respectively, for 1 μM CySH in pH 7.4 PBS. Under this optimized FIA condition, Figure 7A shows the results obtained for different concentrations of CySH in the range of 10 nM to 100 μM. Based on the peak currents in Figure 7A, a linear calibration plot was obtained with a slope and regression coefficient of 0.0788 nA/nM and 0.9999, respectively. Using 10 nM CySH as the test solution, the detection limit (S/N = 3) was 1.70 nM (i.e., 24.22 ng in a 20-μL sample loop). To our knowledge, this is the lowest detection limit ever reported for direct CySH determination without any preliminary accumulation. Thus, by coupling these electrodes with real protein samples, one can certainly get information about the SH quantification and in turn the protein analysis.

The effect of typical organic interferences such as cystine, glucose, and oxalic acid was also studied (Figure 7B). With 10× excess in concentration, only the oxalic acid showed ~20% alteration in the FIA signal of 1 mM CySH. Nevertheless, the FIA signal was very stable when the concentration of interferences was reduced to 5× excess. The sensitivity can certainly be increased provided that pH is <4 in FIA. Furthermore, since the process is diffusion-controlled, the response time for the N*Py*CME is very fast. All the measurements can be done immediately after the N*Py*CME is immersed into the test samples. Finally, no decrease in CySH response, either peak potential or peak current, was observed after the same electrode was repeatedly used and stored in 1.1 M KOH solution for more than 2 months.

CONCLUSIONS

The N*Py*CME showed excellent electrocatalytic effect toward the CySH oxidation. The ac impedance measurements give evidence of the participation of *Py* in the electrocatalytic oxidation process. Studies with standard benchmark systems reveal the unique property of the N*Py*CME. The Michaelis−Menten-type kinetics through the participation of the CyS−*Py*−Ru^{VI} intermediate was well suited for the electrocatalytic oxidation. It is concluded that the SH groups were oxidized effectively on the acidic sites of *Py*. An excellent detection limit was noticed by FIA in the present system. The reliability and stability of the N*Py*CME

(44) Wang, J. *Analytical Electrochemistry*; VCH Publishers: New York, 1994; pp 54−64.

offer a good possibility for extending the technique to routine analysis of CySH in real samples.

ACKNOWLEDGMENT

The authors gratefully acknowledge financial support from the National Science Council of the Republic of China.

Received for review September 11, 2000. Accepted January 12, 2001.

AC0010781